Functional insights of two MATE transporters from *Vibrio fluvialis*

Priyabrata Mohanty[1], Aneri Shah[2] and Ashima Kushwaha Bhardwaj[1]*

1. Department of Human Health and Diseases, Indian Institute of Advanced Research, Koba Institutional Area, Gandhinagar 382 007, Gujarat, India
2. Clinic of Nephrology and Hypertension, Diabetes and Endocrinology, Otto-von-Guericke University Magdeburg, 39120 Magdeburg, Germany

Running title: MATE-type efflux pumps from Vibrio fluvialis

To whom correspondence should be addressed: Dr. Ashima Kushwaha Bhardwaj**,** Department of Human Health and Diseases, Indian Institute of Advanced Research, Koba Institutional Area, Gandhinagar- 382 007, Gujarat, India;
Tel.: + 91 -079-30514235; Fax: + 91 -079-30514110 ; E mail : ashima.bhardwaj@gmail.com

Keywords: Efflux pumps; Recombinant expression; multi-ion dependence; efflux pump inhibition

Summary

Functional characterization of H- and D-MATE (Multidrug and Toxin Extrusion) transporters from clinical isolates of *Vibrio fluvialis* revealed H-type conferred resistance to fluoroquinolones, ethidium bromide and safranin whereas D-type exhibited marginal resistance towards ethidium bromide only. Both H-/D-type transporters were inhibited by reserpine resulting in increased intracellular norfloxacin concentration. The efflux was facilitated by both Na^+/K^+ ions, suggesting that these efflux pumps were ion-dependent. In presence of various classes of EPIs, there was decrease in MIC exhibited by H-/D-type efflux pumps towards norfloxacin which didn't translate into transport inhibition. But reserpine presented a conclusive pattern with decrease in MIC towards norfloxacin and increased norfloxacin accumulation inferring maximum inhibition. Substrate binding and electrostatic charge distribution of both the transporters was similar to other known MATE transporters. The H-type exhibited 10 transmembranes and D-type exhibited 11 TMs which was different from other MATE transporters known to have 12 TMs (Transmembranes). Data derived from molecular docking and ion binding studies revealed that Aspartic Acid residue in 1st TM acts as ion binding site with transport mechanism similar to

NorM. Electrostatic potential map of both the transporters revealed that there is a cavity formation within the transporters surrounded by charged electronegative amino acid residues. Interestingly, surface models of both transporters revealed that 1st TM forms covalent bond with 7th TM towards extracellular space. Docking studies also revealed that reserpine covalently binds to central pocket of both transporters and serves as excellent EPI against these transporters as evidenced by MIC and drug accumulation assays.

Introduction

Resistance mediated by efflux pumps is one of the non-specific mechanisms that pathogenic microbes employ to lower intracellular drug concentration (Bhardwaj & Mohanty, 2012, Van Bambeke *et al.*, 2003, Poole, 2000, Poole, 2004, Poole, 2005). Efflux pumps could be primary transporters utilizing ATP for transport or could be secondary transporters that utilize sodium-/proton-motive force for transport of substrates. Till date six families of transporters are known for their involvement in multidrug resistance (MDR) in prokaryotes (Bhardwaj & Mohanty, 2012, Van Bambeke *et al.*, 2003, Hassan *et al.*, 2015). Multidrug and toxic compound extrusion (MATE) family of efflux pumps is one of the newest and least characterized family of transporters that are proven to be involved in resistance to various antibiotics and dyes including quinolones (Mohanty *et al.*, 2012, Omote *et al.*, 2006). NorM, the prototype member was discovered from *Vibrio parahaemolyticus* (Morita *et al.*, 1998) and subsequently its homologs and orthologs were identified in *Escherichia coli*, *Neisseria gonorrhoeae* and *V. cholerae* (Long *et al.*, 2008, Morita *et al.*, 2000). The MATE family further consists of three protein clusters : the NorM branch involved in MDR, a branch containing several eukaryotic proteins and a branch containing DinF involved in SOS response and MDR (Otsuka *et al.*, 2005). Growing academic interest in this family of transporters is evident from the fact that structures have been solved for a few within a span of last few years from prokaryotic as well as eukaryotic sources(Tanaka *et al.*, 2013, He *et al.*, 2010, Lu *et al.*, 2013b, Lu *et al.*, 2013a, Wong *et al.*, 2014, Tanaka *et al.*, 2017, Miyauchi *et al.*, 2017) . Preliminary *in-silico* and drug

60 transport studies of MATE family of efflux pumps revealed that these efflux pumps are sodium-
61 ion coupled and recognize wide spectrum of substrates but neither of these characteristics have
62 been explicitly explained at molecular level (He *et al.*, 2004). MATE pumps originated from
63 flippases (Meeske *et al.*, 2015). Both MATE and flippases belong to same family of proteins
64 multidrug/oligosaccharidyl-lipid/polysaccharide (MOP) transporter superfamily. Divergence can
65 be seen as functional role has been attributed to aspartic acid in 1st transmembrane of MATE-
66 pumps, which acts as ion binding site whereas serine at 17 position is known to play functional
67 role in MurJ flippases (Kuk *et al.*, 2017). From our laboratory, two MATE-type members (H- and
68 D-) were first identified in *Vibrio fluvialis* (causes cholera-like illness) (Mohanty *et al.*, 2012). The
69 genes were cloned in pBR322 vector and the protein functions were assessed using MIC and
70 drug transport assays. Both the pumps conferred resistance to fluoroquinolones norfloxacin
71 and ciprofloxacin. In the present study, we cloned both the transporters in arabinose promoter-
72 based pBAD vector which allowed visualization of recombinant protein and better control over
73 protein expression. Functional characterization was performed with assays involving MICs, drug
74 uptake and efflux pump inhibitors (EPIs). Molecular docking, ion binding site predictions and
75 surface electrostatics of these transporters using the known MATE-type transporters as
76 reference proteins was carried out to further characterize the functionality of these transporters.

77 **Results and Discussion**

78 ***Expression of recombinant H- and D- MATE-type efflux pumps in E. coli-*** The sequenced
79 genes of D- and H-type efflux pumps were designated as *vcd*, *vfd*, *vch* and vfh, *where* c stands
80 for *V. cholerae* and *f* stands for *V. fluvialis*. Corresponding to each gene, the proteins were
81 designated as VCH, VCD, VFH and VFD. Further the genes were cloned in arabinose driven
82 pBAD expression system and induced as mentioned in materials in methods. Coomassie blue
83 stained gel of arabinose-induced pBAD-*vfd* samples did not show the band corresponding to
84 recombinant VFD at the expected position of 55 kDa (Fig. 1A) whereas the expression of
85 positive control Lac-His was detected at 125 kDa as expected.

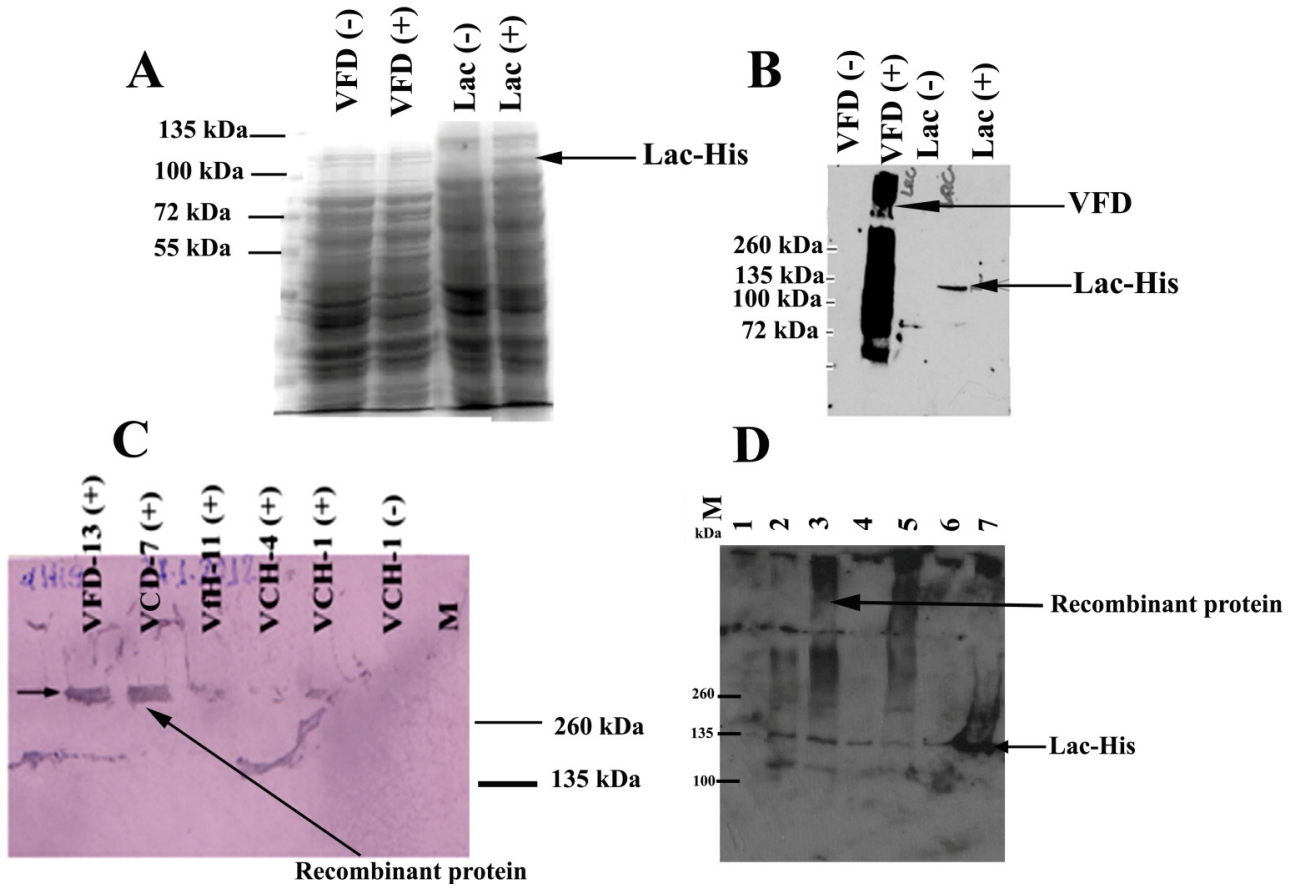

Fig. 1. Total cell expression in induced (+) and uninduced (-) cell lysates of different recombinant pBAD clones. **A.** Coomassie blue stained 10% SDS-PAGE for total cell lysates from pBAD-*vfd* along with pBAD-Lac-His positive control in *E. coli* LMG194; **B.** Western blot of induced (+) and uninduced (-) cell lysates of pBAD-*vfd* along with pBAD-Lac-His positive control. **C.** Western blot of recombinant VCH, VFH, VCD, VFD and Lac-His in LMG194. **D.** Western blot of recombinant proteins in K-12 Δ*tolC*. The cells were induced and developed as described in materials and methods. Lane-1 Prestained Spectramulticolour (Fermentas) molecular weight markers have been indicated on the left of each pane. Lane 2,3,4 and 5 represents VCH, VFH, VCD and VFDFor Panels **B** and **D, the** blots were developed with ECL substrates (Novex, Invitrogen) and for Panel **C**, they were developed with DAB and H_2O_2 Goat Ant-V_5 antibody was used as primary antibody.

Therefore, Western Blot was carried out to determine the expression of recombinant VFD protein with goat anti-V_5 primary antibody and developed with enhanced chemiluminescence substrates. Results revealed the expression of Lac-His positive control at right molecular weight but interesting observation was made in case of pBAD-*vfd*, which showed diffused pattern of bands in the whole lane (Fig 4.16 B). Subsequently, all the four recombinant

105 clones for H- and D-genes were expressed in *E. coli* LMG194 under same conditions. The
106 development of Western blots with goat anti-His antibody using colorimetry clearly depicted a
107 single major band with the mobility greater than 260 kDa in the lanes with induced cells for all
108 the clones (Fig 1 C) . Therefore, the slow development of the Western blots showed single
109 major bands whereas the fast/more sensitive ECL detection could also depict the degradation
110 pattern for the recombinant proteins.
111 Further, all the four recombinant clones for H- and D-genes (*vch*, *vfh*, *vcd* and *vfd*) were
112 expressed in *E. coli* LMG194 and Western blots using colorimetry clearly depicted a single
113 major band with the mobility greater than 260 kDa instead of 55 kDa in the lanes with induced
114 cells for all the clones (Fig. 1C). The sensitivity of ECL led to the visualization of diffused band
115 pattern probably indicating either various stages of oligomerisation/recombinant protein
116 degradation whereas the less sensitive colorimetry showed a single band on Western blot. The
117 diffused band pattern of the recombinant efflux pumps observed in the current study could be
118 the final outcome of aberrant mobility due to oligomerisation. The observed aberrant mobility of
119 recombinant transporter proteins due to oligomerisation has also been reported in case of
120 ammonium transporter AmtB of *E. coli* (Blakey *et al.*, 2002) where the 45 kDa protein showed
121 series of bands of varying molecular weights suggesting it to be an oligomer. In our study, the
122 mobility of the H- and D-recombinant effux pump proteins showed similar pattern on Western
123 blots where ~55 kDa proteins migrated at >260 kDa molecular weight suggesting that the
124 recombinant protein existed as oligomers that were stable in the presence of SDS and β-ME.
125 The recombinant efflux pumps formed a series of aggregated species due to the presence of
126 hydrophobhic patches that appeared as a ladder of high molecular weight bands under
127 denaturing and reducing conditions (Blakey *et al.*, 2002). The wild type Na^+/H^+ antiporter of
128 *Methanococcus jannaschii* presents itself as a dimer even in the presence of SDS and
129 undergoes proteolytic degradation (Goswami *et al.*, 2011). The recombinant expression of
130 membrane proteins is tricky where specialized expression systems have been developed to

131 counteract protein degradation and oligomerisation (Wagner *et al.*, 2008). Taken together, the
132 facts from earlier studies and observations from the present study suggested that H- and D-
133 MATE efflux pumps exhibited aberrant mobility possibly be due to oligomerisation similar to
134 AcrB due to intra-molecular van der Waals bonding that resists dissociation in presence of SDS
135 and β-ME.

136 ***pBAD recombinant efflux pumps are translocated to the membrane-*** Upon successful
137 detection of recombinant proteins in the host cells with aberrant mobility, classical traits of
138 membrane proteins, further studies were carried out to determine if the recombinant proteins
139 were actually targeted to the membrane of the *E. coli* host. Two approaches *i.e.* confocal
140 microscopy and membrane fractionation were utilised to investigate the same.

141 Earlier bioinformatics studies of both the efflux pumps had predicted that these pumps
142 were transmembrane proteins (Mohanty *et al.*, 2012). Localization of these efflux pumps in cell
143 membrane was investigated utilizing confocal microscopy where the laser was programmed to
144 detect membrane marker Film Tracer 1-43 and CY3 fluorochrome conjugated secondary
145 antibody from the same pin hole. Results revealed that VFD and VFH were localised in the
146 membrane of *E. coli* LMG194 (Fig. 2 Panel A: A-F). The recombinant proteins generated red
147 signal due to CY3 (Fig. 2 A, panelsB and E) and membrane marker generated green signal for
148 cell membrane (Fig. 2A,panels A and D). DAPI, which was used for nuclear staining was also
149 employed as counterstain but it did not bind with the nucleoid and was not visible by confocal
150 imaging. Change in the colour of membrane to yellow in the superimposed image of
151 recombinant efflux pump protein and membrane marker (Fig. 2A, panels C and F) suggested
152 that the recombinant proteins were localised in the membrane and were detected by the same
153 pinhole of the microscope.

154

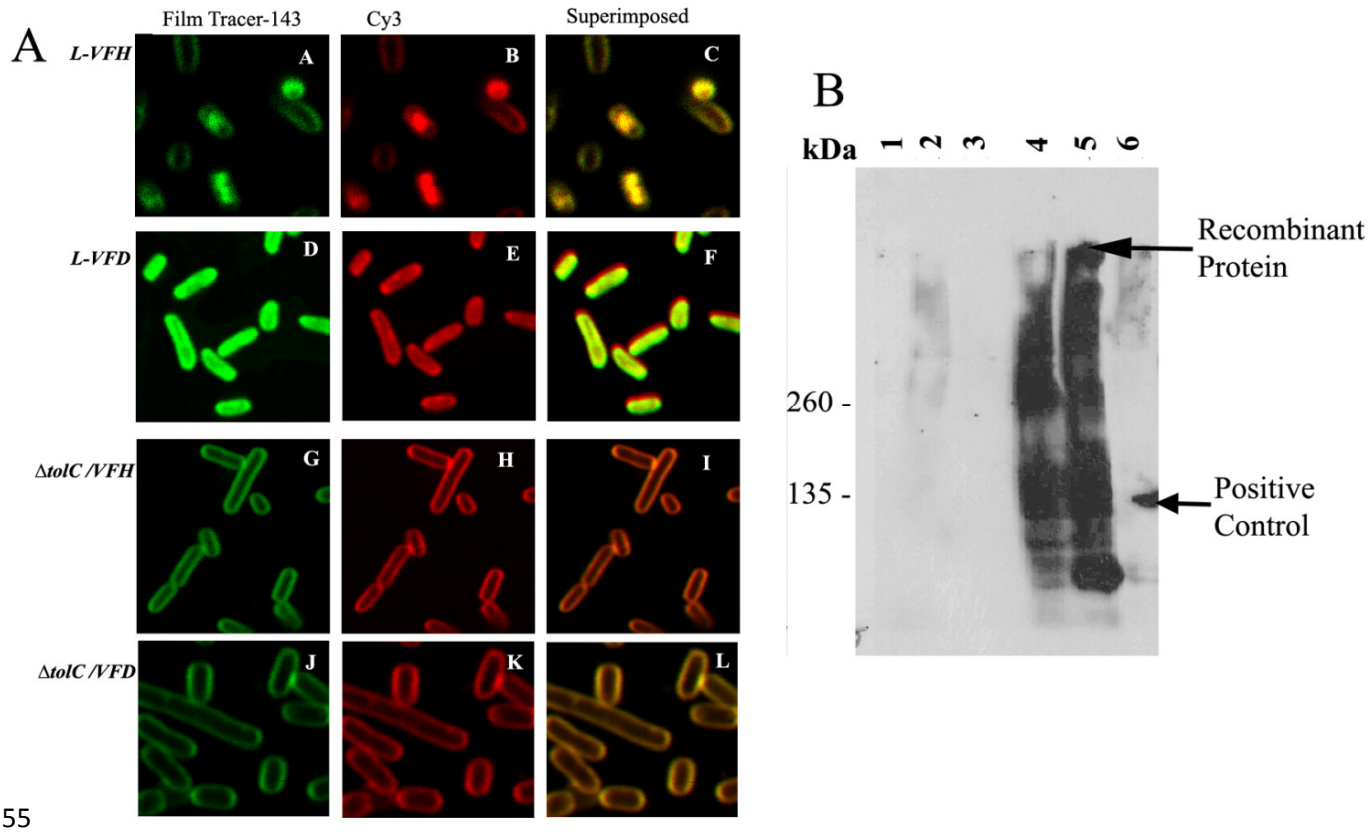

Fig. 2. Membrane localisation of recombinant efflux pumps in *E. coli.* **Panel A.** Confocal imaging of pBAD-recombinants in heterologous *E. coli* host. **A**/**D**:Visualisation of *E. coli* cells harbouring pBAD-*vfh/vfd* stained with membrane marker Film-tracer 1-43; **B**/**E**:Detection of recombinant pBAD-*vfh/vfd* in *E. coli* labelled with Goat anti-Mouse Cy3 secondary antibody; **C**/**F** (63X ZOOM 4): Superimposed/merged images from **A**/**B or D**/**E** of recombinant pBAD-*vfh/vfd* in *E. coli* LMG194; **G**/**J**: Visualisation of *E. coli* cells harbouring pBAD-*vfh/vfd* using membrane marker Film-tracer 1-43; **H**/**K**: Detection of recombinant pBAD-*vfh/vfd* in *E. coli* labelled with Goat anti-Mouse Cy3 secondary antibody; **I**/**L**: Superimposed/merged images from **G**/**H** or **J**/**K** of recombinant pBAD-*vfh/vfd* in *E. coli* K-12 Δ*tolC*2 Δ*tolC*. **Panel B.** Membrane fractionation of *E. coli* harbouring pBAD-*vfd.* 63X Zoom 4 settings were used for obtaining these images. M- Spectramulticolour protein marker (Fermentas). Lane 1- VFD –ve- Total cell lysates for uninduced samples; Lane 2-VFD +ve- Total cell lysates for induced samples; Lane 3- VFD Son (Sup) - total soluble fraction after sonication.; Lane 4- VFD SAR (Sup)- Total soluble proteins after sarkosyl treatment; and Lane 5- VFD SAR Pellet- debris and other subcellular organelles. Lane 6- Lac-HisPositive control. Goat anti-V5 antibody was used as primary antibody. HRP conjugated Mouse Anti-Goat IgG was used as secondary antibody (Jackson Immunoresearch). Prestained Spectramulticolour (Fermentas) molecular weight marker in kDa has been indicated of the left of panel. The blots were developed with Novex ECL substrates (Invitrogen).

To further confirm if the recombinant proteins were localized in the inner membrane, a protocol utilising a combination of membrane fractionation and selective solubilisation of the inner membrane with detergents was employed (Hobb *et al.*, 2009, Leyh, 1990, Frankel *et al.*, 1991).Western blot revealed that upon induction, the recombinant protein was detected in total

178 cell lysate (Fig. 2B, lanes 1 and 2) for VFD. The fraction containing total soluble protein did not
179 show the presence of recombinant protein indicating that the recombinant protein was not
180 cytosolic but probably associated with insoluble fraction (Fig. 2B, lane 3). Sarkosyl solubilised
181 inner membrane fraction (lane 4) revealed the band pattern corresponding to recombinant VFD
182 confirming that the protein was translocated to the inner membrane. This protein was also
183 detected in the sarkosyl treated outer membrane pellet indicating partial solubilisation of the
184 membrane upon sarkosyl treatment (Fig. 2B, lane 5). Apart from the above, partially purified
185 recombinant VFD from inner membrane also showed aberrant migration and diffused band
186 pattern as observed earlier.

187 ***MIC assays for pBAD recombinants in E. coli K-12 ∆tolC indicated different substrate***
188 ***profile for H and D pumps -*** The recombinant constructs for H- and D-type proteins when
189 introduced into *E. coli* LMG194 did not exhibit any change in the MIC against ethidium bromide
190 and norfloxacin although both the compounds had been shown as substrates for these
191 membrane proteins in earlier studies from this laboratory (Mohanty *et al.*, 2012). Earlier studies
192 with pBR322 expression system had utilized *E. coli* host KAM32 with deletion of two major efflux
193 pumps AcrAB and YdhE for functional characterization of the recombinant proteins expressed in
194 this host (Mohanty *et al.*, 2012). In the current study *E. coli* K-12 strains with deletions in genes
195 for major RND efflux systems; ∆*acrA* (deletion of connecting protein), ∆*acrB* (deletion of its
196 inner protein) and ∆*tolC* (deletion of its outer membrane protein) were utilized for functional
197 characterization of pBAD recombinants (Kuroda & Tsuchiya, 2009, Matsuo *et al.*, 2008, Matsuo
198 *et al.*, 2007, Otsuka *et al.*, 2005, Mohanty *et al.*, 2012).

199 Results for MICs of ethidium bromide, ciprofloxacin and norfloxacin showed that though
200 all the three K-12 deletion strains, K-12 ∆*acrA*, K-12 ∆*acrB* and K-12 ∆*tolC* showed reduction in
201 MIC as compared to the control wild type strains K-12 and LMG194, K-12 ∆*tolC* exhibited
202 maximum hypersusceptibilty *i.e.* at least 16-fold decrease in MIC towards ethidium bromide and
203 norfloxacin and more than 8-fold decrease in MIC towards ciprofloxacin (Supplementary Table

204 1). Subsequently, accumulation assays also revealed that *E. coli* K-12Δ*tolC* had the highest
205 drug accumulation in comparison to the other hosts utilised in the study (Supplementary Fig.1).

207 Western blot and confocal microscopy (Fig. 1D and Fig. 2A, panels G to L respectively)
208 revealed that the recombinant proteins were expressed in K-12Δ*tolC* and localized in its inner
209 membrane. Taken together, the results of Western blots, confocal microscopy, MIC and
210 accumulation assays (Supplementary Fig.1) indicated that K-12 Δ*tolC* was a suitable
211 hypersusceptible strain for expression and functional characterization of the recombinant MATE
212 pumps.

213 **Table 1. MIC for recombinant clones carrying MATE-type efflux pump genes from *V.***
214 ***fluvialis* and *V. cholerae* in pBAD expression vector and *E. coli* Δ*tolC* host**

	MIC in µg/mL for the recombinant clones				
Drugs/ Dyes	**Δ*tolC***	**Δ*tolC* /VCH**	**Δ*tolC* /VFH**	**Δ*tolC* /VCD**	**Δ*tolC* /VFD**
Ethidium Bromide	<3.9	**15.6**	**15.6**	**3.9**	**7.8**
Norfloxacin	<0.0156	**0.03125-0.0625**	**0.03125-0.0625**	<0.0156	<0.0156
Ciprofloxacin	<0.00156	**0.003125-0.00625**	**0.003125-0.00625**	<0.00156	<0.00156
Nalidixic Acid	0.3125-0.625	0.3125-0.625	0.3125-0.625	0.3125-0.625	0.3125-0.625
Ofloxacin	0.0125-0.025	0.0125-0.025	0.0125-0.025	0.0125-0.025	0.0125-0.025
Neomycin	>200	200	200	200	200
Gentamicin	3.125	1.56-3.125	3.125	1.56	1.56
Acridine Orange	37.5	37.5	37.5	37.5	37.5
Acriflavin	6.25	**12.5**	**12.5**	6.25	6.25
Safranin	3.125	**12.5**	**12.5**	3.125	3.125

215
216 As kanamycin cassette is inserted in place of the gene of interest (Δ*tolC*) to be disrupted, so MIC against
217 kanamycin could not be evaluated against pBAD recombinants in Δ*tolC* . Increase in MIC is shown as
218 bold.

219 Subsequently, *E. coli* K-12 Δ*tolC* expressing pBAD recombinants for VFH, VCH, VFD
220 and VCD presented an interesting profile in terms of recognition/transport by these two pumps
221 (Table 1). H-type pumps exhibited increase in MIC for ethidium bromide (at least 4-fold),
222 norfloxacin and ciprofloxacin (atleast 2-4-fold), acriflavin (2-fold) and safranin (4-fold). As
223 against this, D-type pumps conferred resistance only towards ethidium bromide with at least 2-

224 fold increase in MIC when compared to the control. Both H- and D-type pumps showed almost
225 similar/slight decrease (2-fold) in MIC for the aminoglycosides (neomycin and gentamicin). Both
226 H- and D-type pumps showed unaltered MIC for nalidixic acid, ofloxacin and acridine orange
227 while D-type pumps additionally showed unaltered MIC for norfloxacin, ciprofloxacin, acriflavin
228 and safranin.

229 NorM, the prototype member of MATE-type efflux pumps from *V. parahaemolyticus* is a
230 broad spectrum efflux pump reported to confer resistance towards basic lipophilic compounds
231 like ethidium bromide and rhodamine, hydrophilic aminoglycosides like kanamycin and
232 neomycin and hydrophilic zwitterionic fluoroquinolones such as norfloxacin and ciprofloxacin,
233 but not to hydrophobic quinolones such as sparfloxacin and nalidixic acid (Morita *et al.*, 1998).
234 In the present study, H-type recombinant seemed to be an efflux pump with primary transport
235 capability towards zwitterionic fluoroquinolones and basic lipophilic compounds. Earlier studies
236 had revealed that H-type pumps (VCH/VFH) exhibited resistance towards norfloxacin and
237 ciprofloxacin only when expressed in pBR322 expression system (Mohanty *et al.*, 2012) but
238 when these pumps were expressed in pBAD/Δ*tolC* system, they exhibited norfloxacin and
239 ciprofloxacin resistance along with extended resistance towards ethidium bromide, acriflavin
240 and safranin. The expression of efflux pumps is generally very low and results in a modest
241 increase of two-four folds in MIC (Long *et al.*, 2008) which was also observed in the current
242 study (Long *et al.*, 2008). KetM from *Klebsiella pneumoniae* also exhibited narrow spectrum
243 resistance to fluoroquinolones with modest change in MIC (Ogawa *et al.*, 2015). Asp32, Glu251
244 and Asp367 from *V. parahaemolyticus* NorM were implicated in sodium-dependent transport of
245 antimicrobials and Asp32 specifically is known for its role in efflux thus conferring resistance
246 towards norfloxacin and ethidium bromide (Otsuka *et al.*, 2005). Even though the efflux pumps
247 in the present study carried only Asp at position 40/38 in TM1 out of three conserved residues
248 they were able to exhibit marginal MDR phenotype. This also gives a notion that apart from
249 these three amino acids, other residues might play important role in transport. It was later

250 proven in MATE transporter from the plant *Camelina sativa* (Tanaka *et al.*, 2017). Glutamic
251 Acid , glutamine, asparagine, arginine along with aspartic acid amino acid residues were
252 implicated for their role in forming hydrophobic cavity formation and transport in MATE
253 transporter from the plant *Camelina sativa* (Tanaka *et al.*, 2017).

254 ***Accumulation assays revealed that the recombinant strains were able to efflux***
255 ***drugs/dyes-*** The substrate transport studies revealed that there was an increased
256 accumulation of ethidium bromide by pBAD recombinants expressing either H-/D-type efflux
257 pumps in comparison with control as also observed in earlier studies with their corresponding
258 pBR322 recombinants (Mohanty *et al.*, 2012) (Fig. 3A and 3B).

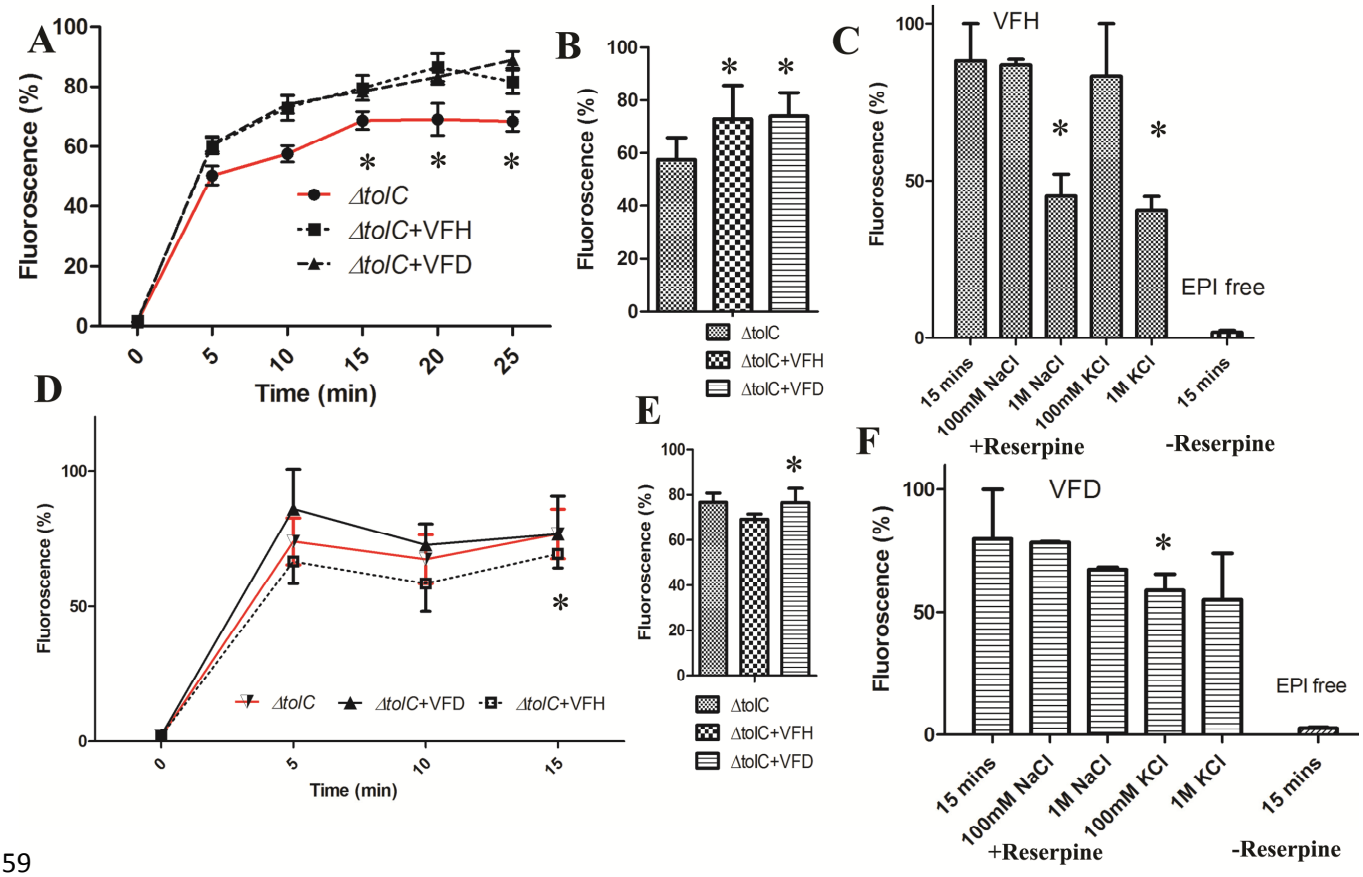

259

260 **Fig. 3**. **A/D.** Intracellular ethidium bromide/norfloxacin accumulation in recombinant K-12 Δ*tolC*
261 harbouring *vfd* and *vfh* genes in pBAD vector. Samples were collected at every 5 mins for processing
262 and fluorescence was measured A/**B.** Intracellular ethidium bromide accumulation in recombinant K-12
263 ΔtolC harbouring *vfd* and *vfh* genes in pBAD vector after 15 mins. D/**E.** Intracellular norfloxacin
264 accumulation in recombinant K-12 ΔtolC harbouring *vfd* and *vfh* genes in pBAD vector after 15 mins. **C/F.**
265 Ion dependence of pBAD recombinant efflux pumps in the presence of 100 mM or 1 M sodium chloride
266 (NaCl) or 100 mM or 1 M potassium chloride (KCl) in K-12 ΔtolC cells transformed with *pBAD-vfh/vfdVFD*.

267 Data is expressed as mean percentage fluorescence intensity of the maximum fluorescence intensity
268 obtained during the experiment from three independent experiments and * represents significant
269 difference to control ($P < 0.05$).

270 The intracellular ethidium bromide accumulation profiles of both the efflux pumps was in
271 contrast to the results of MIC assays where elevation in MIC was observed towards ethidium
272 bromide (Fig. 3A and 3B; Table 2). The absence of correlation between the results of MIC and
273 accumulation assays particularly in ethidium bromide could result due to the time period of both
274 the assays.

275 However, in case of norfloxacin, there was a correlation between MIC assays and
276 accumulation assays. Results revealed that recombinants with H-type pumps which exhibited
277 increased MIC towards norfloxacin, showed lowering of intracellular norfloxacin accumulation
278 whereas recombinants harbouring D-type efflux pumps that exhibited unaltered susceptibility
279 towards norfloxacin showed almost similar intracellular norfloxacin concentration as compared
280 to the control (Fig. 3D and 3E). Subsequently ion dependence assays were performed for both
281 the transporters to understand their fueling mechanism.

282 ***The Na^+/K^+-ions equally facilitated the efflux of norfloxacin by H- pumps -*** Earlier studies
283 from our laboratory as well as others had revealed that MATE pumps belonging to NorM cluster
284 could transport their substrates in the presence of monovalent ions like Na^+ (Morita *et al.*, 1998,
285 Mohanty *et al.*, 2012). The K-12 Δ*tolC/* pBAD-*vfh* recombinants were loaded with norfloxacin in
286 the presence of reserpine, a compound known to block efflux activity. Subsequently, different
287 concentrations of 0.1 M and 1 M NaCl or KCl were added to the assay mixture and intracellular
288 norfloxacin was monitored to assess the effect of these ions on the efflux activity of these
289 pumps. Results showed that there was an increase in intracellular norfloxacin accumulation in
290 this recombinant in the presence of reserpine compared to reserpine free control (Fig. 3C and
291 3F, columns 1 and 6 respectively). Though the addition of 100 mM KCl/NaCl did not
292 significantly induce the efflux, increase in salt concentration to 1M KCl/NaCl resulted in a

293 greater efflux of the drug from these cells compared to the cells without any salts (Fig. 3C and
294 3F, columns 2-5).

295 Earlier studies on MATE- efflux pumps had established that these efflux pumps were
296 fueled either by Na^+/H^+-ions for transport (Bhardwaj & Mohanty, 2012) which was also observed
297 in the current study. There was an increase in intracellular drug concentration in H-
298 recombinants when the Efflux Pump Inhibitor (EPI) reserpine was added. Effluxing commenced
299 on addition of Na^+/ K^+ ions. Newer studies also point out that the transport capability of MATE-
300 type *E. coli* ClbM transporter involved in transport of precolibactin was equally influenced by
301 Na^+, K^+ and Rb^+ ions (Mousa *et al.*, 2017). K^+ ions are known to be congener of Na^+ ions.
302 Another study revealed that NorM from *V. parahaemolyticus* utilises both PMF and Na^+ for
303 transport (Jin *et al.*, 2014). Overall it seems both the transporters are Na^+-ion dependent which
304 has been proved earlier (Mohanty *et al.*, 2012).

305 ***Changes in MIC of norfloxacin in the presence of EPIs-*** Different types of EPIs were utilised
306 to deduce actual transport mechanism of these efflux pumps.. For this, the MIC of these EPIs
307 was deduced against host *E. coli* K-12 Δ*tolC* and sub-lethal concentrations of EPIs (~50% of
308 MIC) were utilized to monitor changes in MIC/drug accumulation patterns for recombinant efflux
309 pumps.

310 Results revealed that compounds like FCCP and CCCP were effective at low
311 concentrations to host and with norfloxacin a decrease in MIC was observed for H-type (at least
312 8-folds) and for D-type (2 folds) Table 2). Both compounds are known to kill living cells at low
313 concentration as they disrupt PMF, and have been extensively utilised for inhibition of efflux
314 pumps with concentrations varying for each study (Begum *et al.*, 2005, Morita *et al.*, 2000,
315 Morita *et al.*, 1998). Other compounds like DNP which deplete ATP or compounds like NIG, NA
316 and VAL which are known as H^+, Na^+ and K^+ specific ionophores respectively, exhibited high
317 MIC for host. But with norfloxacin, DNP and NIG also decreased the MIC by at least 2-8-folds
318 for norfloxacin. against both the compounds (Table 2). VAL and NA did not inhibit both the

319 **Table 2. Change in MICs of norfloxacin in pBAD recombinant clones carrying MATE-type**
320 **efflux pump genes from *V. fluvialis* and *V. cholerae* with addition of EPIs**

Substrate/EPI	**Strain/ clones**				
Nor	**ΔtolC**	**ΔtolC /VCH**	**ΔtolC /VFH**	**ΔtolC /VCD**	**ΔtolC /VFD**
Nor	<0.0156	0.03125-0.0625	0.03125 -0.0625	<0.0156	<0.0156
+CCCP	**<0.0078**	**<0.0078**	**<0.0078**	**<0.0078**	**<0.0078**
+FCCP	**<0.0078**	**<0.0078**	**<0.0078**	**<0.0078**	**<0.0078**
+RES	**<0.0078**	**<0.0078**	**<0.0078**	**<0.0078**	**<0.0078**
+NEM	**<0.0078**	**<0.0078**	**<0.0078**	**<0.0078**	**<0.0078**
+DNP	**<0.0078**	**<0.0078**	**<0.0078**	**<0.0078**	**<0.0078**
+VAL	0.0625	0.0625	0.0625	0.03125	0.0625
+NIG	**<0.0078**	**<0.0078**	**<0.0078**	**<0.0078**	**<0.0078**
+NA	0.03125-0.0625	0.03125-0.0625	0.03125	0.0156-0.03125	0.0625

321 Carbonyl cyanide-p-trifluoromethoxyphenyl hydrazone (FCCP), Carbonyl cyanide m-chlorophenyl
322 hydrazone (CCCP), Nigericin (NIG), Valinomycin (VAL), N-ethyl maleidamide (NEM), Dintrophenol
323 (DNP), Reserpine (RES), Sodium Ionophore (NA), Norfloxacin (Nor). The concentration of EPIs used in
324 µg/mL are FCCP 3.125, CCCP 1.56, NIG 50, VAL 50, NEM 62.5, DNP 25, RES 125 and NA 50.
325

326 pumps for norfloxacin (Table 2). These ionophores mostly increase transferability of ions across
327 membrane involved in generating EMF, which may or may not be important for energy recycling
328 (Castro *et al.*, 2015). RES and NEM, both of which either bind or covalently modify the efflux
329 pumps, also exhibited very high MIC for *E. coli* K-12 ΔtolC but in conjunction with norfloxacin,
330 both compounds decreased the MIC (Table 2). Both NEM and RES decreased the MIC
331 exhibited by both pumps by at least 2-16-folds whereas (Table 2). It was not surprising that
332 reserpine increased sensitivity towards fluoroquinolones. Resperine had been earlier reported to
333 inhibit various efflux pumps resulting in increased susceptibility (Baranova & Neyfakh, 1997,
334 Brenwald *et al.*, 1997, Aeschlimann *et al.*, 1999, Markham, 1999, Markham *et al.*, 1999,
335 Gibbons & Udo, 2000, Mullin *et al.*, 2004).

337 ***Accumulation of norfloxacin by H-/D-type pumps in the presence of EPIs-*** The MIC assays
338 had established that some of the EPIs were active in reducing the MIC of norfloxacin for the

339 recombinants expressing efflux pumps. Therefore, norfloxacin accumulation studies were
340 performed to assess the real time effect on drug transport by the H-/D- recombinants in the
341 presence/absence of EPIs.
342 Results revealed that *E. coli* K-12 Δ*tolC* expressing H-type pumps showed a marginal to
343 moderate degree of increased norfloxacin accumulation in presence of CCCP and FCCP in
344 comparison to EPI free control (Fig. 4). These pumps exhibited almost unaltered/marginal
345 increased accumulation of norfloxacin in presence of NIG, NEM, VAL and DNP (Fig. 4).
346 Interestingly, both efflux pumps exhibited very high accumulation of norfloxacin in presence of
347 RES (Fig. 4). MIC studies of norfloxacin against both recombinants in the presence of EPIs had
348 revealed that compounds like CCCP, RES and FCCP decreased the MICs (Table 4). This was
349 in sync to the norfloxacin accumulation results, where these compounds increased the
350 accumulation of norfloxacin. NA increased the intracellular norfloxacin for H-type of efflux which
351 was in contrast to MIC assays where it did not decrease the MIC for norfloxacin (Table 2).
352 However, for NEM, DNP and NIG this correlation between MIC and accumulation results
353 was missing probably due to the kinetics of inhibition by these EPIs and the difference in the
354 time course for the two type of assays. MATE family of efflux pumps utilise Na^+ ions for
355 transport which was observed in the current study. There was an increased intracellular
356 norfloxacin accumulation with utilisation of H^+/ Na^+/K^+ ion specific ionophores such as NA,
357 CCCP and FCCP. This was in corroboration with our earlier observation in ion dependence
358 experiments where we observed that both the efflux pumps showed greater efflux in presence
359 of both Na^+ and K^+ ions also evidenced in MIC experiments (Table 2) where these EPIs
360 decreased the MIC of norfloxacin. Taken together, there was a relative correlation between drug
361 accumulation, ion dependence and change in MIC patterns in case of some selected EPIs.
362

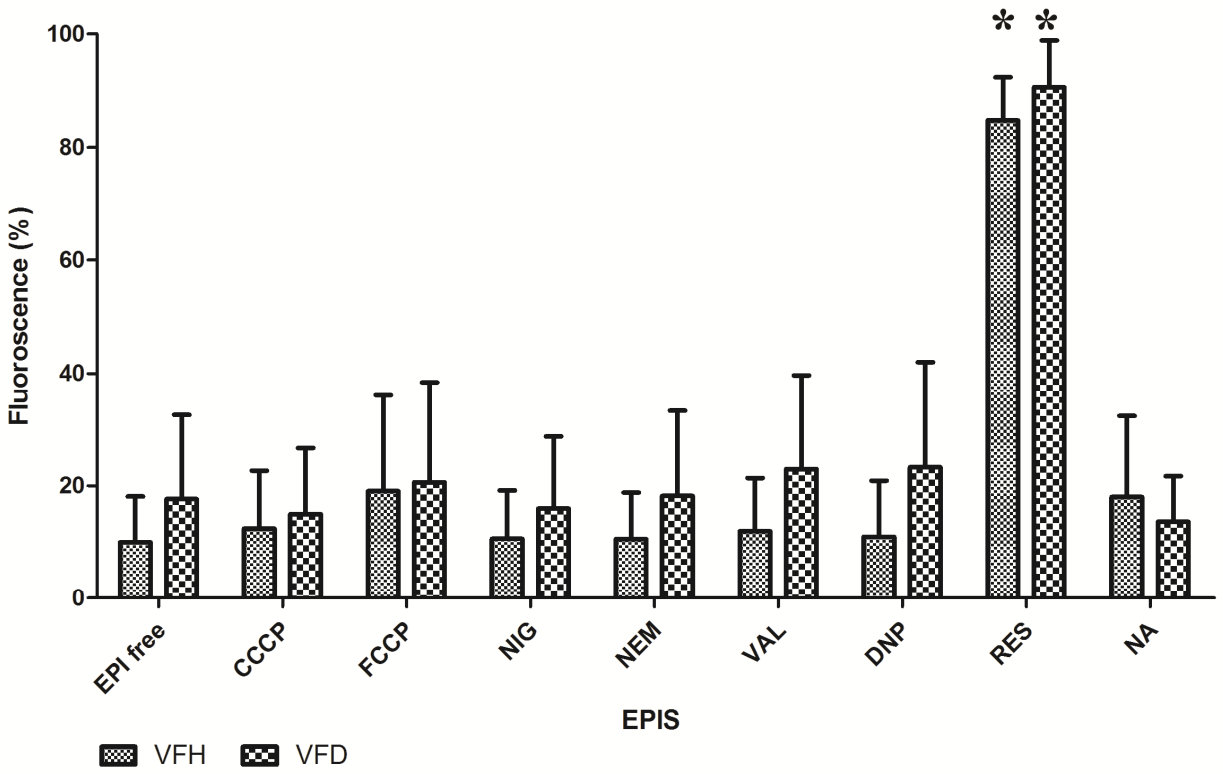

363

364 **Fig. 4.** Accumulation of norfloxacin in presence of various EPIs. Accumulation of norfloxacin by *E. coli* K-
365 12 Δ*tolC* expressing H- and D-type pumps in the presence of EPIs. Recombinant *E. coli* K-12 ΔtolC was
366 loaded with norfloxacin and incubated at 37℃ for 15 mins in presence/absence of EPIs. These samples
367 were subsequently processed and analyzed for fluorescence intensity as described in the materials and
368 methods. * represents significant difference to control ($P < 0.05$). The concentration of EPIs used in
369 µg/mL are FCCP 3.125, CCCP 1.56, NIG 50, VAL 50, NEM 62.5, DNP 25, RES 125 and NA 50.
370

371 **Molecular Modeling and docking-** Structural prediction of MATE-type efflux pumps had
372 suggested 12 transmembrane helices in their structure which was further validated with the
373 structure of first Na^+ dependent MATE-type efflux pump from *Pyrococcus furiosus* having 12
374 transmembranes (Lomovskaya & Bostian, 2006, Tanaka *et al.*, 2013). In our earlier attempt in
375 predicting 3D structures of VFH and VFD using I-TASSER server, we had reported that VFD
376 had 11 transmembranes (TMs) whereas VFH had 10 TMs (Mohanty *et al.*, 2012). After 2012,
377 more structures were solved for the members of this family of transporters (Tanaka *et al.*, 2013,
378 He *et al.*, 2010, Lu *et al.*, 2013b, Lu *et al.*, 2013a). Subsequent to these studies, further attempts
379 for protein modeling were made using SwissModel (https://swissmodel.expasy.org/).to

380 understand the topology and mechanism of efflux by these two MATE pumps Both PyMol
381 (https://pymol.org/2/) and Chimera (https://www.cgl.ucsf.edu/chimera/) were used
382 forvisualization of their molecular structures. Results revealed that both the efflux pumps had 10
383 predicted TMs arranged in two bundles of 5 TMs each (Fig. 5.) similar to crystal structures of
384 earlier published MATE transporters (Lu *et al.*, 2013b).

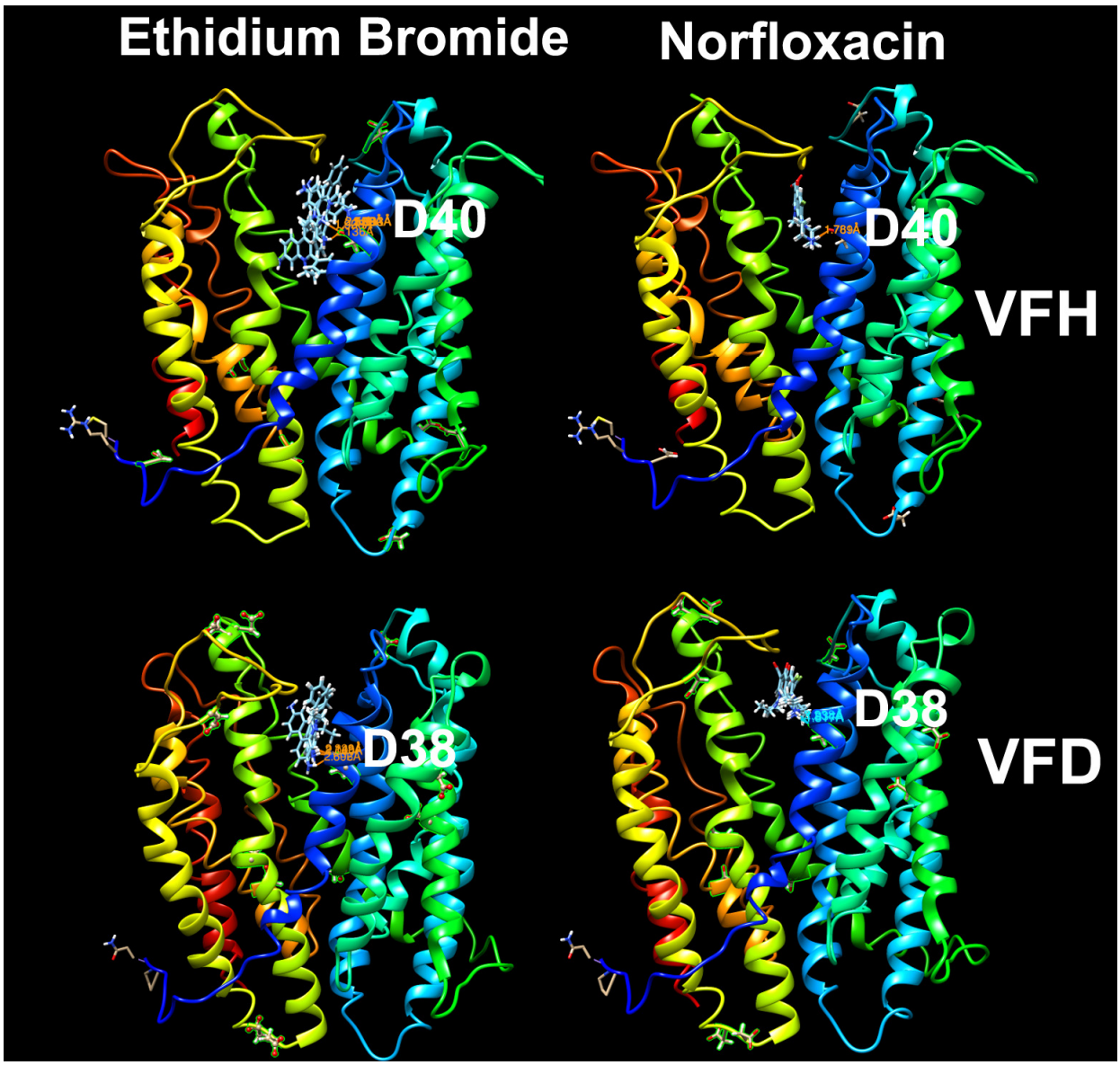

385

386 **Fig. 5.** Docked pose of ethidium bromide and Norfloxacin with *V. fluvialis* MATE efflux pumps (VFH and
387 VFD) forming covalent complex at Asp 38/40 of 1st transmembrane.

388 They were also outward facing like NorM (Lu *et al.*, 2013b) with distinct internal cavity. It was
389 both in corroboration (for VFH) and contrast (for VFD) to our earlier finding where VFH model
390 was similar to NorM and VFD had different predicted protein model (Mohanty *et al.*, 2012).
391 Subsequently, molecular docking was done using SwissDock (http://www.swissdock.ch/) to
392 validate binding interactions of both the transporters with ethidium bromide and norfloxacin as
393 both the transporters showed certain degree of transport for these substrates. Classically, a
394 MATE pump has 12 TMs arranged in two bundles of six TMs each (Tanaka *et al.*, 2013,
395 Tanaka *et al.*, 2017, Radchenko *et al.*, 2016, Lu *et al.*, 2013b).

396 Table 3 **Ligand-docking of VFH and VFD efflux pumps with various substrates**

Protein	**Substrate**	**Orientation**	**Total Binding sites**	**Total Hydrogen Bonding**	**Most plausible binding site**
VFH	Nor	Outward	35 clusters with 256 binding sites	11 clusters with 65 sites	1 cluster with 6 binding sites (deltag -8.4)
VFH	EtBr	Outward	30 clusters with 256 binding sites	10 clusters with 69 sites	3 clusters with 20 binding sites (deltag -6.9)
VFD	Nor	Outward	35 clusters with 256 binding sites	23 clusters with 139 sites	1 cluster with 8 binding sites (deltag -7.4 to -7.5)
VFD	EtBr	Outward	34 clusters with 256 binding sites	15 clusters with 80 sites	2 clusters with 10 binding sites (deltag -7.19)

397

398 The first TM has an ion binding site represented by D32, the Aspartic Acid residue at 32
399 position (Otsuka *et al.*, 2005, Long *et al.*, 2008, Lu *et al.*, 2013a, Lu *et al.*, 2013b). With this
400 input, the protein sequences of both the transporters were submitted to SwissDock ≈server
401 (http://www.swissdock.ch/). The docking was programmed for finding all possible ligand
402 interactions. All aspartic acid residues were first identified from the generated models and
403 hydrogen bonds were calculated. The details have been presented in Table 3 and Fig 5.

404 Interaction between the protein and ligands was optimum in the first TM at D40 for VFH and
405 D38 for VFD which was similar to earlier published findings (Tanaka *et al.*, 2013, He *et al.*,
406 2010, Lu *et al.*, 2013b, Lu *et al.*, 2013a). This also indicated similar transport mechanism for
407 both the transporters. Both the compounds ethidium bromide and norfloxacin fitted well in the
408 central cavity of both the transporters. The only noticed difference was that while norfloxacin
409 fitted in a straight fashion forming bonds with D40/38, Ethidium bromide showed bent fitting from
410 1st to 7th TM (Fig. 5).

412 **Ion binding and Electrostatic potential surface representation-** MATE-type efflux pumps are
413 secondary pumps that utilize Na^+/H^+ for transport (Jin *et al.*, 2014, Mohanty *et al.*, 2012). Earlier
414 studies had proved that these were Na^+ ion-driven transporters (Mohanty *et al.*, 2012). In the
415 ion-dependence assays, we observed the transport capability was equally influenced by both
416 sodium and potassium ions for VFH (reference). For better understanding of ion dependence
417 and amino acid residues involved, we utilized IonCom server
418 (https://zhanglab.ccmb.med.umich.edu/IonCom/) to predict their ion dependence and amino
419 acid residues involved.

420 Results revealed that both the efflux pumps had no binding site detected for the
421 following ions:(Cu, Fe, Ca, Mg, Mn, Na, K, CO, NO_2, SO_4, PO_4). The predicted ion binding
422 amino acid residues were D40, E51, Q82, D88, Y138, H163, N179, N309 and D393 for VFH
423 and D38, H44, W49, Q81, N163 and D204 for VFD. Interestingly, docking studies clearly
424 indicated that D38/40 of both the transporters were involved in binding. So, even though we
425 couldn't predict dependence of ion but D38/40 seems most plausible ion binding site for both
426 the transporters which was similar to NorM from *V. cholerae* (He *et al.*, 2010).

427 Electrostatic potential of proteins is caused by charged amino acid residues in side
428 chains, bound or unbound by various ions and play various roles such as protein folding and
429 stability and function of the proteins. APBS pluggin in PyMol was used to calculate the
430 electrostatic potential for both the proteins. It may reflects secondary and tertiary structures of

431 transporters and their affinity to bind to substrates. Results revealed that both VFH and VFD
432 had different hydrophobicity patches similar to other known MATE transporters (Fig 6a) (Zheng
433 *et al.*, 2018). Both VFH and VFD formed a central cavity surrounded by charged electronegative
434 amino acids. VFH also had an electropositive centre at the end of the cavity (Fig 6a).
435 Subsequently, VFH and VFD with all possible interaction with norfloxacin via docking were
436 mapped along and electrostatic potential was calculated, an interesting scenario came out. A
437 sizable norfloxacin molecule was assembled in the cavity of VFH whereas fewer norfloxacin
438 molecules were assembled in the cavity Of VFD. NorM which was taken as control had
439 maximum norfloxacin molecules assembled in the cavity (Fig 6c). This was in sync with our
440 earlier observation where VFH exhibited broader transport capability than VFD in MIC. The
441 arrangement was mostly concentrated towards n-lobe which was similar like NorM (Lu *et al.*,
442 2013a)

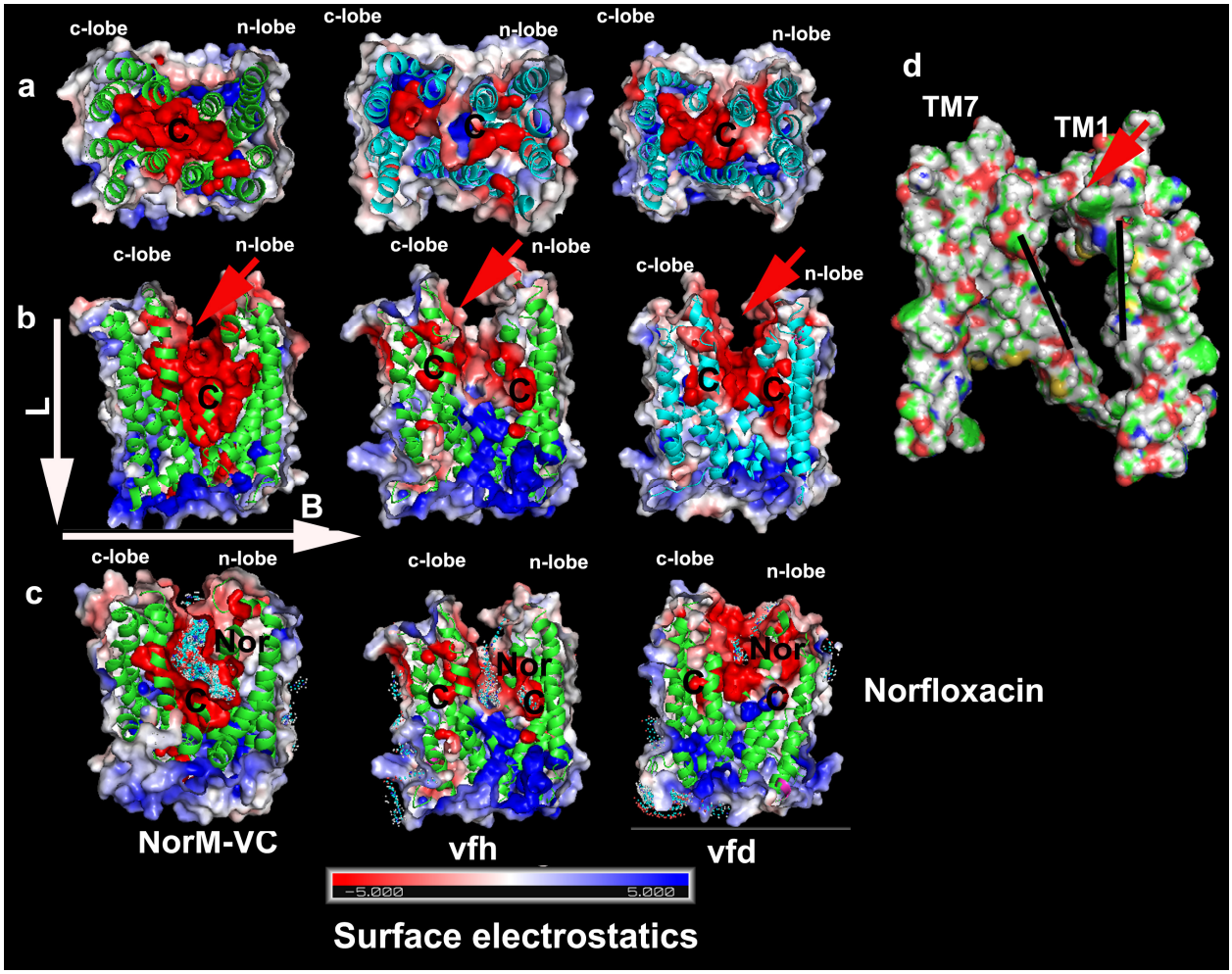

Fig. 6. Surface charge differences between VFH, VFD and NorM-VC. Surface electrostatics were calculated by the APBS plugin in PyMOL. Cross-section model of VFH, VFD and NorM-VC surface representation is shown from the membrane region (a) or from the extracellular (b) sides (c) with norfloxacin and (d) Cross-section model of VFH/VFD exposing covalent interaction between TM1 and TM7. C represents cavity. Red arrows represent cavity.

It has been widely accepted that MATE transporters evolved from genetic duplication of flippases (Lomovskaya & Bostian, 2006, Tanaka *et al.*, 2013). Comparison of both the transporters with known structures of MATE transporters from *Camelina sativa,* NorM from *Vibrio cholarae* and MurJ flippases from *Thermosipho africanus* reveals interesting similarities and divergence from both VFH and VFD. D38/40 of both the transporters seemed to more conserved in bacterial transporters (Lu *et al.*, 2013b, He *et al.*, 2010) in comparison to their eukaryotic counterparts (Tanaka *et al.*, 2017). When both these transporters were compared to their evolutionary predecessors like MurJ (Kuk *et al.*, 2017), the difference is quite significant.

458 MurJ flippases from *Thermosipho africanus* exhibited presence of 14 TMs arranged in 6+6
459 similar to bacterial transporters and functional role of last two TMs is unknown. Ser17, Arg18,
460 Arg24, Arg52, and Arg255 in 1st Tm of Murj has been proved important for recognizing the
461 diphosphate and/or sugar moieties of lipid II whereas Asp in 1st Tm of NorM has been proved for
462 ion dependence and substrate transport (He *et al.*, 2010). It seems both VFH and VFD has
463 similar topology like NorM with presence of D38/40 in 1st TM creating a hydrophobic cavity for
464 substrate recognition and transport.

465 During mapping of electrostatic potential of VFH and VFD, an aberrant architecture was
466 also observed in both the transporters. MATE transporters usually have 12 TMs arranged in two
467 bundles with 6 TMS each. Each forms one lobe and are usually free. The 1st TM upon
468 protonation displaces to 7th TM to facilitate transport. But in case of both VFH/VFD, the loop
469 connecting 1st TM to 2nd TM forms a covalent structure with loop of 7th TM connecting 8th TM as
470 elucidated by surface model (Fig 6d). MATE type transporters are thought to be evolved of
471 internal genetic duplication, resulting in two lobes. VFH/VFD had 10 TMs, still there was greater
472 scope for transport. The formation of covalent bond reduces mobility of 1st TM to be displaced
473 to 6th TM and may overall hinder transport efficiency (Fig 7b).

474 **Mechanism of inhibition of both the transporters by reserpine-** Our earlier observation with
475 electrostatic mapping and inhibition of both the transporters with various EPIs had led to an
476 indication that the transport of norfloxacin was indeed hampered in presence of these EPIs.
477 Surprisingly, the similar effect couldn't be observed in case of drug transport assay. Compounds
478 like CCCP/FCCP, which are extremely toxic to cell at low concentration showed marginal
479 inhibition. Reserpine which was fairly non-toxic, was able to inhibit both the transporters in real
480 time drug transport assays. In our earlier study, we had observed 20 microgram/mL was
481 sufficient to inhibit both the transporters (Mohanty *et al.*, 2012). Even in the current study, the
482 MIC against the host was fairly high i.e >128 mcg/mL. So, range of concentration was quite
483 enough to inhibit. Even thoughit has been earlier proved in case of Bmr transporters, where

484 certain residues were implicated for inhibition (Klyachko *et al*., 1997), no direct structural studies
485 have ever proved the actual inhibition by reserpine in MATE efflux pump. To investigate the
486 exact nature, we tried to dock reserpine with both the transporters along with NorM from *V.*
487 *cholerae*.

488 Results revealed that reserpine could conveniently fit into electronegative cavities of
489 both the transporters. VFH had 3 binding clusters with 19 binding sites whereas VFD had 2
490 binding clusters with 15 binding sites. Interestingly, NorM had 26 binding clusters with 190
491 binding sites.

492 In some of the earlier studies, MATE transporters have been co-crystalized along with
493 the inhibitors. (Tanaka *et al*., 2013) . These studies have delineated the role of hydrogen
494 bonding between transportersand ligand for exact inhibition mechanism. Our own observation
495 with NorMhad hinted the same as there were almost 15 clusters and 96 binding sites forming
496 hydrogen bonds in the cavity of NorM. But in case of VFH there was no predicted hydrogen
497 bond formation and for VFD, 1 cluster and 3 binding site configuration was observed. Previous
498 studies regarding co-crystallization of MATE-transporters with certain inhibitors had shed light
499 on formation of electrostatic bonds for inhibition with verapamil and macrocyclic peptides
500 (Radchenko *et al*., 2015, Tanaka *et al*., 2013). Observation from our earlier studies and current
501 study reflect that reserpine acts pretty well at different concentrations also.

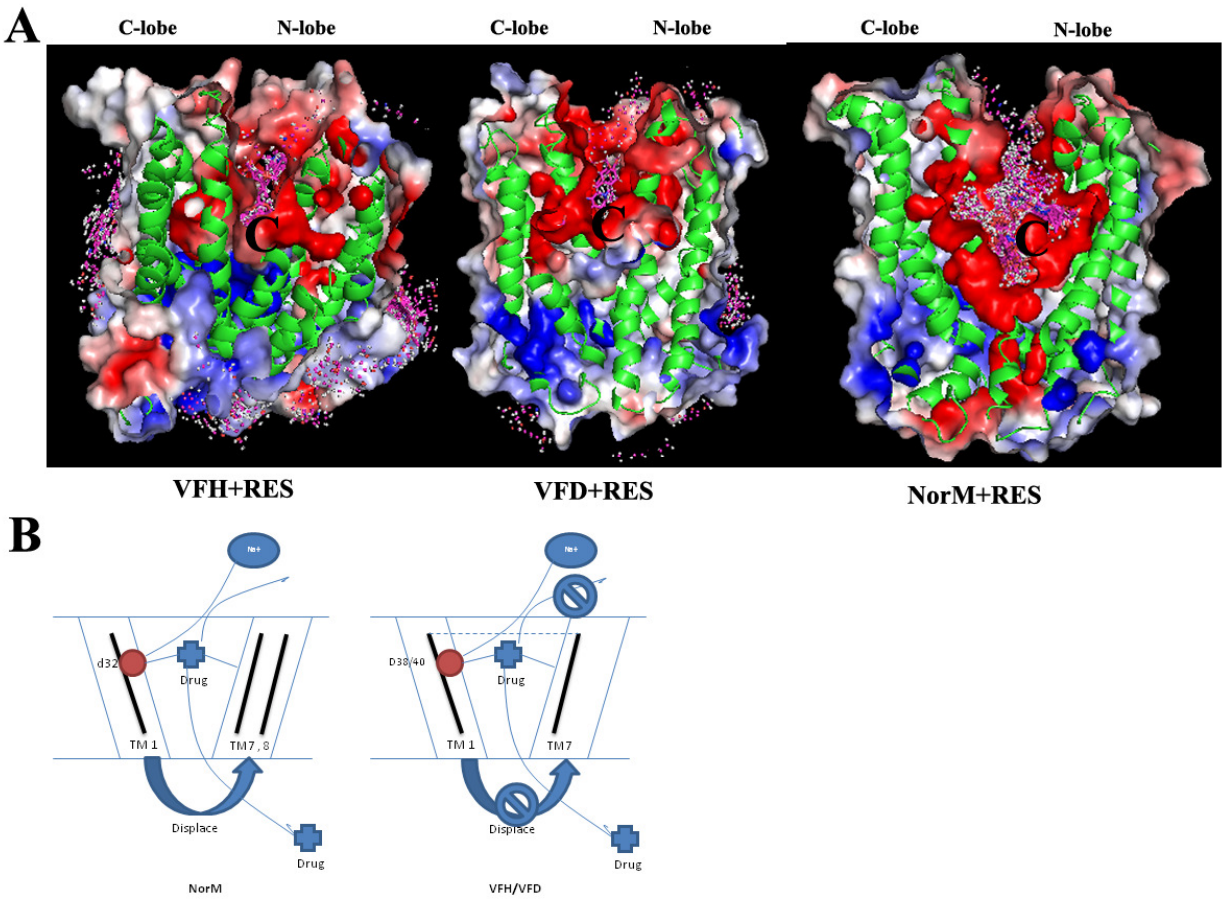

Fig. 7. A. Docked pose of reserpine with *V. fluvialis* MATE efflux pumps (VFH and VFD) . **B.** Proposed mechanism of transport of NorM-VC and VFD/VFH. Contrasting to NorM-VC, VFH/VFD forms covalent interactions between TM1 and TM7, which along low cavity volume leads to low transport capability of VFH/VFD.

The exact mechanism of reserpine inhibition is binding to phenylalanine, tryptophan and tyrosine residues of Bmr efflux pumps (Steinfels *et al.*, 2004) and inhibition by reserpine does not involve ion bioenergetics of the cell and seems to be a non-specific inhibition of efflux pumps as was also seen in the current study. This led us to believe three important aspects of transport a. mobility of each lobe plays a vital role in transport b. size and electronegativity of central cavity plays important role for actual substrate recognition c. binding of ligand in electronegative pocket is not always electrostatic but may be covalent as reserpine was able to inhibit without actual hydrogen bond formation in both the transporters.

516 **Experimental procedures**

517 ***Cloning in pBAD-TOPO-TA vector-*** The primers used for cloning in pBAD vectors were VFH-
518 BAD-F/VFH-BAD-R and VFD-BAD-F/VFD-BAD-R mentioned in supplementary table 2. The
519 amplicons were subsequently purified using PCR purification kit (Qiagen) and ligated in pBAD
520 vector (Invitrogen) according to manufacturer's protocol.

521 ***Expression and detection of recombinants harbouring pBAD efflux pump genes-*** pBAD
522 clones for expression of VCH, VFH, VCD and *VFD* (where D- and H- are two MATE-type efflux
523 pumps, VC stands for *V. cholerae* and VF stands for *V. fluvialis*) and Lac-His (positive control)
524 were transformed in *E. coli* LMG194 and *E. coli* K-12 Δ *tolC* (JW5503-1, *E. coli* Genetic
525 Resource Centre, Yale University) for expression as well as functional characterization. For
526 Western blots, *E. coli* LMG194/K12 Δ*tolC* cells transformed with the recombinant vectors were
527 grown in Luria-Bertani (LB) medium to an optical density of 0.5 at 600 nm (OD_{600}) and induced
528 with 0.2% L-arabinose for 4 hours and the total cell lysates prepared in SDS-PAGE lysis buffer
529 were electrophoresed on 8% SDS-PAGE. Western blot was done with 0.45 micron
530 nitrocellulose membrane (Whatman/Pall Life sciences) and blocked with 5% fat free milk
531 powder in Tris buffered saline with 0.05% tween 20 (TBST) for 2 hours at room temperature.
532 The blot was incubated with goat Anti-His/V_5 primary antibody at 1:5000 dilutions in 0.5% milk
533 powder in TBST for 2 hours at room temperature with constant shaking followed by washing in
534 TBST and incubation with anti-Goat IgG-HRP (Horseradish Peroxidase)/Anti-Goat IgG-AP
535 (Alkaline Phosphatase) (Jackson Immunoresearch) secondary antibody. The blots were
536 developed either by using Novex ECL HRP chemiluminiscent development kit (Invitrogen) or by
537 colorimetry using DAB/H_2O_2 (for HRP conjugated secondary antibody) or BCIP/NBT
538 (Calbiochem) (for AP conjugated secondary antibody) according to the manufacturer's
539 instructions. For chemiluminiscence, the blot was dried and developed on X-ray.

540

541 ***Detection of expression of recombinant proteins by confocal imaging-*** Briefly, the cells
542 were grown and induced as discussed in earlier subsection of Experimental Procedures. 200 µL
543 of induced cells were centrifuged at 5000 rpm for 5 min, the cells were resuspended in 50 µL of
544 supernatant and were spotted on coverslips coated with 0.2% L-Poly-lysine (Sigma) in 24-well
545 tissue culture plates (Corning) for 30 min at room temperature. Cells were then fixed using 4%
546 paraformaldehyde (PFA) for 15 min followed by washing twice with 250 µL PBST (PBS
547 containing 0.05% Tween 20) for 5 min without shaking. The cells were blocked with 5% Bovine
548 Serum Albumin (BSA) in PBST for 1 hour at room temperature followed by washing thrice with
549 500 µL PBST for 10 min each and solutions were aspirated gently using a pipette. 50 µL mouse
550 monoclonal anti-6X His tagged primary antibody (Calbiochem) was added at a dilution of 1:150
551 in 0.5 % BSA in PBST in the respective wells and incubated for 2 hours without shaking at room
552 temperature. Washing was done thrice as described above. Goat anti-mouse secondary
553 antibody labeled with Cy3 (Invitrogen) was added at the dilution of 1: 50 in 0.5 % BSA in PBST
554 and incubated for 2 hours at room temperature followed by one washing step. Cells were
555 counterstained with 200 µL of 4', 6-diamidino-2-phenylindole (DAPI) at 1 µg mL^{-1} concentration
556 and 50 µL of Film Tracer 1-43 membrane marker (Invitrogen) at 1 µg mL-1 concentration in
557 DMSO. Confocal imaging was carried out using CTR 6500 confocal microscope (Leica). Diode
558 lamp was utilised for detection of DAPI, UV HeNe lamp for CY3 and Argon lamp was used to
559 detect membrane marker.

560 ***Preparation of Membrane fraction-*** The membrane fraction was prepared according to the
561 published protocol (Leyh, 1990). The *E. coli* LMG194/ K12 Δ*tolC* recombinant cells were grown
562 and induced as described earlier. 25 mL of induced cultures were harvested at 5000 rpm, 4℃
563 for 15 min. The supernatant was discarded and the pellet was washed with 5 mL ice cold PBS
564 (phosphate-buffered saline) followed by centrifugation at 5000 rpm, 4℃ for 10 min. The cells
565 were resuspended in 1 mL lysis buffer (50 mM potassium phosphate, pH 7.8) having 1 mM
566 phenylmethanesulfonyl fluoride and incubated in -80℃ deep freezer for 2 hours. The samples

567 were then thawed and sonicated 4 times with 30 sec on and off pulse on ice. The samples were
568 then centrifuged at 8000 rpm, 4℃ for 5 min. The supernatants were saved as soluble fraction
569 and the pellet was treated with 200 µL of 2% sarcosyl solution (Sigma Aldrich) and incubated at
570 room temperature for 30 min. The sample was then centrifuged at 15,000 rpm for 30 min at
571 room temperature to obtain inner membrane proteins as supernatant and the rest of the proteins
572 as pellet. Samples were subsequently subjected to Western blot for detection of recombinant
573 proteins.

574 ***Minimum Inhibitory Concentration (MIC) assays-*** The pBAD expression clones *of vfh*, *vch*,
575 *vcd* and *vfd* were transformed in *E. coli* LMG194/K-12 Δ*tolC* cells, grown in LB broth containing
576 ampicillin (100 µg mL^{-1}) to an OD_{600} of 0.5 and induced with 0.2% L-arabinose for 4 hours.
577 Kanamycin (30 µg mL^{-1}) was additionally used for *E. coli* K-12 Δ*tolC* cells. Drugs/dyes were
578 serially double diluted in LB broth containing 0.2% L-arabinose and 2 mL dilution/well were
579 dispensed in 24 well tissue culture plates (Corning). OD_{600} of the induced sample was adjusted
580 to 0.08-0.13 and 50 µL of this sample was added to each well. Incubation was done at 37℃.
581 Readings were observed visually after 16 hours. The assays were repeated at least three times.

582 ***Drug/Dye accumulation assays-*** For *E. coli* K-12ΔtolC cells harboring either pBAD-*vfh* or
583 pBAD-*vfd* or not harbouring any plasmids were grown and induced as described earlier in
584 Materials and methods. Ethidium bromide (1.9 µg mL^{-1}) and norfloxacin (0.0156 µg mL^{-1}) were
585 used for accumulation assays. This was followed by single washing with 0.1 M Tris.HCl, pH 7.0
586 and resuspension in equal volume of the same buffer. The samples were collected every 15
587 min. The processing of the cells and monitoring of the fluorescent content was carried out
588 exactly as described earlier (Mohanty *et al.*, 2012).

589 ***Effect of Na^+/K^+ ions on efflux of drugs/dyes-*** *E. coli* K-12Δ*tolC* cells harboring either *pBAD-*
590 *vfh* or *pBAD-vfd* or not harbouring any plasmids were grown in LB broth containing kanamycin
591 (30 µg mL^{-1}) and induced with 0.02% L-arabinose for 4 hours. Ampicillin was only added to the

592 cells harbouring recombinant plasmids. The recombinants were grown and processed as
593 described above in this section. The samples were then harvested by centrifugation, washed
594 thrice with buffer containing 0.1M Tris.HCl, pH 7.0, and suspended in the same buffer to an
595 OD_{600} of 1.0. The drug/dyes were used at 50% of the MIC values for transport studies.
596 Norfloxacin at a final concentration of 0.0156 µg mL^{-1} (50% MIC concentration)along with 125
597 µg mL^{-1} of reserpine was added to the cell suspension and incubated for 30 min at 37℃. After
598 30 min, 1 mL samples were collected and stored in prechilled microcentrifuge tubes. Negative
599 control (without drug/dyes) and EPI free control were also included in the study. Appropriate
600 volume of 5 M and 0.5 M NaCl/KCl stock solution were added to assay mixture to a final
601 concentration of 1M and 100 mM, incubated at 37℃ for 15 minutes and 1 mL sample was
602 collected. The volume was kept constant irrespective of salt concentration. Samples were then
603 centrifuged at 10,000 rpm for 5 min at 4℃, washed once with 0.1 M Tris.HCl, pH 7.0 buffer and
604 resuspended in 1 mL of 100 mM glycine.HCl, pH 3.0. These samples were subsequently
605 processed and analyzed for fluorescence intensity as described in the previous sections. The
606 maximum fluorescence observed in the experiment was considered to be 100%.

607 ***Assays to determine efficacy of various EPIs on recombinant efflux pumps-*** The MIC of
608 various EPIs was deduced against *E. coli* K-12 Δ*tolC*.Different concentrations of EPIs were
609 prepared by two-fold dilution method in LB broth containing kanamycin (30 µg mL^{-1}) and 100
610 µL/well was dispensed in 96-well tissue culture plates (Corning Inc.). The EPIs were procured
611 from Sigma Aldrich. *E. coli* K-12 Δ*tolC* was grown in LB containing kanamycin (30 µg mL^{-1}) to
612 an OD_{600} of 0.08-0.13. Five microlitre of cells were inoculated in 100 µL medium containing
613 various concentrations of EPIs in a 96 well plate. Observations were made visually after 16
614 hours. The experiments were repeated at least thrice. 50% concentration of MIC of each EPI
615 was utilised in combination with various concentrations of norfloxacin. The *E. coli* K-12 Δ*tolC*
616 carrying recombinant efflux pump plasmids and control *E. coli* K-12 Δ*tolC* were each grown in
617 LB with kanamycin (30 µg mL^{-1}) and ampicillin (100 µg mL^{-1}). Overnight primary cultures were

done in same way. Then 10 mL of secondary culture was prepared. Upon reaching OD_{600} of 0.5, the cells were induced with 0.02% L-arabinose for 4 hours with 200 rpm shaking at 37°C. The optical density of induced cells were adjusted to 0.08-0.13. Five microlitre of cells were inoculated in 100 µL medium containing 50% concentration of various EPIs along with various concentrations of norfloxacin in a 96 well plate (Corning Inc). Observations were made visually after 16 hours. The experiments were repeated at least thrice. The change in MIC was noted to observe efficacy of each EPI.

Acknowledgments: The authors thank Indian Council of Medical Research, New Delhi for providing Senior Research Fellowship to PM (F/815/2011/ECD-II), Department of Biotechnology, New Delhi for Junior Research Fellowship (BT/PR/ 11634 INF/22/104/2008) of AS, Dr. A.K. Tiwari, Department of Developmental Biology, IIAR for helping in confocal imaging and the Puri Foundation for Education in India for support.

Author contributions: Conceived and designed the experiments: AKB and PM. Performed the experiments: PM AS AKB. Analyzed the data: AKB PM. Contributed reagents/materials/analysis tools: AKB. Wrote the paper: AKB PM.

Conflict of interest: The authors declare that they have no conflicts of interest.

Reference

Aeschlimann, J.R., L.D. Dresser, G.W. Kaatz & M.J. Rybak, (1999) Effects of NorA inhibitors on in vitro antibacterial activities and postantibiotic effects of levofloxacin, ciprofloxacin, and norfloxacin in genetically related strains of Staphylococcus aureus. *Antimicrob Agents Chemother* **43**: 335-340.

Baranova, N.N. & A.A. Neyfakh, (1997) Apparent involvement of a multidrug transporter in the fluoroquinolone resistance of Streptococcus pneumoniae. *Antimicrob Agents Chemother* **41**: 1396-1398.

Begum, A., M.M. Rahman, W. Ogawa, T. Mizushima, T. Kuroda & T. Tsuchiya, (2005) Gene cloning and characterization of four MATE family multidrug efflux pumps from Vibrio cholerae non-O1. *Microbiol Immunol* **49**: 949-957.

Bhardwaj, A. & P. Mohanty, (2012) Bacterial efflux pumps involved in multidrug resistance and their inhibitors: rejuvinating the antimicrobial chemotherapy. *Recent patents on anti-infective drug discovery* **7**: 73-89.

Blakey, D., A. Leech, G.H. Thomas, G. Coutts, K. Findlay & M. Merrick, (2002) Purification of the Escherichia coli ammonium transporter AmtB reveals a trimeric stoichiometry. *Biochem J* **364**: 527-535.

651 Brenwald, N.P., M.J. Gill & R. Wise, (1997) The effect of reserpine, an inhibitor of multi-drug
652 efflux pumps, on the in-vitro susceptibilities of fluoroquinolone-resistant strains of
653 Streptococcus pneumoniae to norfloxacin. *The Journal of antimicrobial chemotherapy*
654 **40**: 458-460.
655 Castro, P.J., A.F. Silva, B.C. Marreiros, A.P. Batista & M.M. Pereira, (2015) Respiratory
656 complex I: A dual relation with H and Na? *Biochim Biophys Acta*.
657 Frankel, S., R. Sohn & L. Leinwand, (1991) The use of sarkosyl in generating soluble protein
658 after bacterial expression. *Proc Natl Acad Sci U S A* **88**: 1192-1196.
659 Gibbons, S. & E.E. Udo, (2000) The effect of reserpine, a modulator of multidrug efflux pumps,
660 on the in vitro activity of tetracycline against clinical isolates of methicillin resistant
661 Staphylococcus aureus (MRSA) possessing the tet(K) determinant. *Phytotherapy*
662 *research : PTR* **14**: 139-140.
663 Goswami, P., C. Paulino, D. Hizlan, J. Vonck, O. Yildiz & W. Kuhlbrandt, (2011) Structure of the
664 archaeal Na+/H+ antiporter NhaP1 and functional role of transmembrane helix 1. *Embo*
665 *J* **30**: 439-449.
666 Hassan, K.A., Q. Liu, P.J. Henderson & I.T. Paulsen, (2015) Homologs of the Acinetobacter
667 baumannii AceI transporter represent a new family of bacterial multidrug efflux systems.
668 *MBio* **6**.
669 He, G.X., T. Kuroda, T. Mima, Y. Morita, T. Mizushima & T. Tsuchiya, (2004) An H(+)-coupled
670 multidrug efflux pump, PmpM, a member of the MATE family of transporters, from
671 Pseudomonas aeruginosa. *J Bacteriol* **186**: 262-265.
672 He, X., P. Szewczyk, A. Karyakin, M. Evin, W.X. Hong, Q. Zhang & G. Chang, (2010) Structure
673 of a cation-bound multidrug and toxic compound extrusion transporter. *Nature* **467**: 991-
674 994.
675 Hobb, R.I., J.A. Fields, C.M. Burns & S.A. Thompson, (2009) Evaluation of procedures for outer
676 membrane isolation from Campylobacter jejuni. *Microbiology* **155**: 979-988.
677 Jin, Y., A. Nair & H.W. van Veen, (2014) Multidrug transport protein norM from vibrio cholerae
678 simultaneously couples to sodium- and proton-motive force. *J Biol Chem* **289**: 14624-
679 14632.
680 Klyachko, K.A., S. Schuldiner & A.A. Neyfakh, (1997) Mutations affecting substrate specificity of
681 the Bacillus subtilis multidrug transporter Bmr. *Journal of bacteriology* **179**: 2189-2193.
682 Kuk, A.C., E.H. Mashalidis & S.Y. Lee, (2017) Crystal structure of the MOP flippase MurJ in an
683 inward-facing conformation. *Nat Struct Mol Biol* **24**: 171-176.
684 Kuroda, T. & T. Tsuchiya, (2009) Multidrug efflux transporters in the MATE family. *Biochim*
685 *Biophys Acta* **1794**: 763-768.
686 Leyh, R.D., (1990) Characterization of the outer membrane proteins of Bordetella avium. In:
687 Veterinary Microbiology and Preventive Medicine. Ames: Iowa State University, pp. 115.
688 Lomovskaya, O. & K.A. Bostian, (2006) Practical applications and feasibility of efflux pump
689 inhibitors in the clinic--a vision for applied use. *Biochemical pharmacology* **71**: 910-918.
690 Long, F., C. Rouquette-Loughlin, W.M. Shafer & E.W. Yu, (2008) Functional cloning and
691 characterization of the multidrug efflux pumps NorM from Neisseria gonorrhoeae and
692 YdhE from Escherichia coli. *Antimicrob Agents Chemother* **52**: 3052-3060.
693 Lu, M., M. Radchenko, J. Symersky, R. Nie & Y. Guo, (2013a) Structural insights into H+-
694 coupled multidrug extrusion by a MATE transporter. *Nat Struct Mol Biol* **20**: 1310-1317.
695 Lu, M., J. Symersky, M. Radchenko, A. Koide, Y. Guo, R. Nie & S. Koide, (2013b) Structures of
696 a Na+-coupled, substrate-bound MATE multidrug transporter. *Proc Natl Acad Sci U S A*
697 **110**: 2099-2104.
698 Markham, P.N., (1999) Inhibition of the emergence of ciprofloxacin resistance in Streptococcus
699 pneumoniae by the multidrug efflux inhibitor reserpine. *Antimicrob Agents Chemother*
700 **43**: 988-989.

701 Markham, P.N., E. Westhaus, K. Klyachko, M.E. Johnson & A.A. Neyfakh, (1999) Multiple novel
702 inhibitors of the NorA multidrug transporter of Staphylococcus aureus. *Antimicrobial*
703 *agents and chemotherapy* **43**: 2404-2408.
704 Matsuo, T., J. Chen, Y. Minato, W. Ogawa, T. Mizushima, T. Kuroda & T. Tsuchiya, (2008)
705 SmdAB, a heterodimeric ABC-Type multidrug efflux pump, in Serratia marcescens. *J*
706 *Bacteriol* **190**: 648-654.
707 Matsuo, T., K. Hayashi, Y. Morita, M. Koterasawa, W. Ogawa, T. Mizushima, T. Tsuchiya & T.
708 Kuroda, (2007) VmeAB, an RND-type multidrug efflux transporter in Vibrio
709 parahaemolyticus. *Microbiology* **153**: 4129-4137.
710 Meeske, A.J., L.T. Sham, H. Kimsey, B.M. Koo, C.A. Gross, T.G. Bernhardt & D.Z. Rudner,
711 (2015) MurJ and a novel lipid II flippase are required for cell wall biogenesis in Bacillus
712 subtilis. *Proc Natl Acad Sci U S A* **112**: 6437-6442.
713 Miyauchi, H., S. Moriyama, T. Kusakizako, K. Kumazaki, T. Nakane, K. Yamashita, K. Hirata, N.
714 Dohmae, T. Nishizawa, K. Ito, T. Miyaji, Y. Moriyama, R. Ishitani & O. Nureki, (2017)
715 Structural basis for xenobiotic extrusion by eukaryotic MATE transporter. *Nat Commun*
716 **8**: 1633.
717 Mohanty, P., A. Patel & A. Kushwaha Bhardwaj, (2012) Role of H- and D- MATE-type
718 transporters from multidrug resistant clinical isolates of Vibrio fluvialis in conferring
719 fluoroquinolone resistance. *PloS one* **7**: e35752.
720 Morita, Y., A. Kataoka, S. Shiota, T. Mizushima & T. Tsuchiya, (2000) NorM of vibrio
721 parahaemolyticus is an Na(+)-driven multidrug efflux pump. *J Bacteriol* **182**: 6694-6697.
722 Morita, Y., K. Kodama, S. Shiota, T. Mine, A. Kataoka, T. Mizushima & T. Tsuchiya, (1998)
723 NorM, a putative multidrug efflux protein, of Vibrio parahaemolyticus and its homolog in
724 Escherichia coli. *Antimicrob Agents Chemother* **42**: 1778-1782.
725 Mousa, J.J., R.C. Newsome, Y. Yang, C. Jobin & S.D. Bruner, (2017) ClbM is a versatile,
726 cation-promiscuous MATE transporter found in the colibactin biosynthetic gene cluster.
727 *Biochem Biophys Res Commun* **482**: 1233-1239.
728 Mullin, S., N. Mani & T.H. Grossman, (2004) Inhibition of antibiotic efflux in bacteria by the novel
729 multidrug resistance inhibitors biricodar (VX-710) and timcodar (VX-853). *Antimicrob*
730 *Agents Chemother* **48**: 4171-4176.
731 Ogawa, W., Y. Minato, H. Dodan, M. Onishi, T. Tsuchiya & T. Kuroda, (2015) Characterization
732 of MATE-Type Multidrug Efflux Pumps from Klebsiella pneumoniae MGH78578. *PloS*
733 *one* **10**: e0121619.
734 Omote, H., M. Hiasa, T. Matsumoto, M. Otsuka & Y. Moriyama, (2006) The MATE proteins as
735 fundamental transporters of metabolic and xenobiotic organic cations. *Trends Pharmacol*
736 *Sci* **27**: 587-593.
737 Otsuka, M., M. Yasuda, Y. Morita, C. Otsuka, T. Tsuchiya, H. Omote & Y. Moriyama, (2005)
738 Identification of essential amino acid residues of the NorM Na+/multidrug antiporter in
739 Vibrio parahaemolyticus. *Journal of bacteriology* **187**: 1552-1558.
740 Poole, K., (2000) Efflux-mediated resistance to fluoroquinolones in gram-negative bacteria.
741 *Antimicrob Agents Chemother* **44**: 2233-2241.
742 Poole, K., (2004) Efflux-mediated multiresistance in Gram-negative bacteria. *Clinical*
743 *microbiology and infection : the official publication of the European Society of Clinical*
744 *Microbiology and Infectious Diseases* **10**: 12-26.
745 Poole, K., (2005) Efflux-mediated antimicrobial resistance. *The Journal of antimicrobial*
746 *chemotherapy* **56**: 20-51.
747 Radchenko, M., R. Nie & M. Lu, (2016) Disulfide Cross-linking of a Multidrug and Toxic
748 Compound Extrusion Transporter Impacts Multidrug Efflux. *J Biol Chem* **291**: 9818-9826.
749 Radchenko, M., J. Symersky, R. Nie & M. Lu, (2015) Structural basis for the blockade of MATE
750 multidrug efflux pumps. *Nat Commun* **6**: 7995.

751 Steinfels, E., C. Orelle, J.R. Fantino, O. Dalmas, J.L. Rigaud, F. Denizot, A. Di Pietro & J.M.
752 Jault, (2004) Characterization of YvcC (BmrA), a multidrug ABC transporter
753 constitutively expressed in Bacillus subtilis. *Biochemistry* **43**: 7491-7502.
754 Tanaka, Y., C.J. Hipolito, A.D. Maturana, K. Ito, T. Kuroda, T. Higuchi, T. Katoh, H.E. Kato, M.
755 Hattori, K. Kumazaki, T. Tsukazaki, R. Ishitani, H. Suga & O. Nureki, (2013) Structural
756 basis for the drug extrusion mechanism by a MATE multidrug transporter. *Nature* **496**:
757 247-251.
758 Tanaka, Y., S. Iwaki & T. Tsukazaki, (2017) Crystal Structure of a Plant Multidrug and Toxic
759 Compound Extrusion Family Protein. *Structure* **25**: 1455-1460 e1452.
760 Van Bambeke, F., Y. Glupczynski, P. Plesiat, J.C. Pechere & P.M. Tulkens, (2003) Antibiotic
761 efflux pumps in prokaryotic cells: occurrence, impact on resistance and strategies for the
762 future of antimicrobial therapy. *J Antimicrob Chemother* **51**: 1055-1065.
763 Wagner, S., M.M. Klepsch, S. Schlegel, A. Appel, R. Draheim, M. Tarry, M. Hogbom, K.J. van
764 Wijk, D.J. Slotboom, J.O. Persson & J.W. de Gier, (2008) Tuning Escherichia coli for
765 membrane protein overexpression. *Proc Natl Acad Sci U S A* **105**: 14371-14376.
766 Wong, K., J. Ma, A. Rothnie, P.C. Biggin & I.D. Kerr, (2014) Towards understanding promiscuity
767 in multidrug efflux pumps. *Trends Biochem Sci* **39**: 8-16.
768 Zheng, S., L.T. Sham, F.A. Rubino, K.P. Brock, W.P. Robins, J.J. Mekalanos, D.S. Marks, T.G.
769 Bernhardt & A.C. Kruse, (2018) Structure and mutagenic analysis of the lipid II flippase
770 MurJ from Escherichia coli. *Proc Natl Acad Sci U S A* **115**: 6709-6714.

771

772

773

774